2011 American Control Conference
on O'Farrell Street, San Francisco, CA, USA
June 29 - July 01, 2011

Optimal Catalyst Temperature Management of Plug-in Hybrid Electric Vehicles

Dongsuk Kum, Huei Peng, and Norman K. Bucknor

Abstract—**For driving cycles that require use of the engine (i.e. the trip distance exceeds the All Electric Range (AER) of a Plug-in Hybrid Electric Vehicle (PHEV) or a driving cycle demands power exceeding the battery peak power), the catalyst temperature management for reduced tailpipe emissions is a challenging control problem due to the frequent and extended engine shut-down and catalyst cool-down. In this paper, we develop a method to synthesize a supervisory powertrain controller (SPC) that achieves near-optimal fuel economy and tailpipe emissions under known travel distances. We first find the globally optimal solution using dynamic programming (DP), which provides an optimal control policy and state trajectories. Based on the analysis of the optimal state trajectories, a variable Energy-to-Distance Ratio (EDR) is introduced to quantify the level of battery state-of-charge (SOC) relative to the remaining distance. A novel two-dimensional extraction method is developed to extract engine on/off, gear-shift, and power-split control strategies as functions of both EDR and the catalyst temperature from the DP control policy. Based on the extracted results, an adaptive SPC that optimally adjusts the engine on/off, gear-shift, and power-split strategies under various EDR and catalyst temperature conditions was developed to achieve near-optimal fuel economy and emission performance.**

I. Introduction

RECENTLY, Plug-in Hybrid Electric Vehicles (PHEVs) received much attention as a promising technology to lower ground transportation's dependency on petroleum fuel and to reduce CO_2 emissions. The dramatic reduction in fossil fuel consumption of the PHEV is achieved by substituting fossil fuels with grid electricity. As an example, when the All Electric Range (AER) of a PHEV is 30 miles, in theory it will be possible to use little or no fossil fuel when the travel distance is less than 30 miles, assuming the electric power source is capable of satisfying the propulsion power need. When the trip distance exceeds AER, and especially when emissions are considered, the optimal control of the PHEV is non-trivial–an optimal supervisory powertrain controller (SPC) that minimizes fuel consumption while maintaining catalyst temperature high for various trip distances is difficult to design. In this study, we seek to develop a systematic method for the synthesis of the SPC to achieve near-optimal fuel economy (FE) and emission performance regardless of trip distances, assuming that the trip distance information is available. If not available, one of the best and simplest strategies would be to use the vehicle's average daily trip distance.

The focus of past PHEV control studies has been on how to use the available battery energy efficiently throughout the driving cycle when the travel distance exceeds the AER. Gonder and Markel proposed and compared three control strategies, electric vehicle/charge sustaining (EV/CS), engine-dominant, and electric-dominant strategy [1]. They found fuel economy is sensitive to travel distances and driving conditions, and suggested that the control strategy should be switched from one to another to improve FE based on the future driving information. A study by Sharer *et al*. performed similar analysis on EV/CS, full engine power, and optimal engine power strategies and reached similar conclusions [2]. When emissions are considered, the optimal control of the PHEV becomes much more complex because the PHEV is designed to dramatically reduce fuel consumption by frequent and extended engine shut-down. A recent study by the authors developed a systematic design method of an SPC that achieves near-optimal fuel economy for a PHEV [3]. In this paper, we build upon that work by applying the design method for PHEVs.

II. Plug-in Hybrid Electric Vehicle Model

A. Target PHEV

The target vehicle is a compact SUV with the pre-transmission parallel hybrid configuration (Fig. 1). An engine-disconnect clutch replaces the torque converter for pure electric vehicle (EV) mode. Main design variables of the PHEV are battery capacity and rated power of the battery and motor/generator (M/G). In this study, the same battery capacity and electric propulsion power of the previous study is

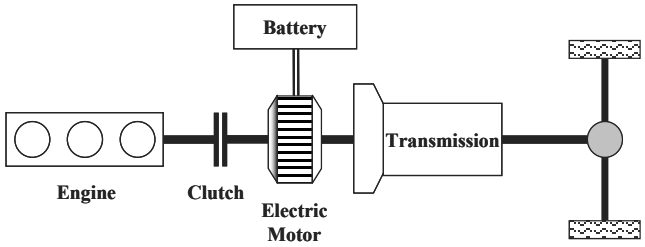

Fig. 1. Schematic of a pre-transmission parallel hybrid electric vehicle powertrain.

This work was supported by the General Motors.

Dongsuk Kum is with the General Motors R&D Center, Warren, MI 48090 USA (e-mail: dongsuk.kum@gm.com).

Huei Peng is with the Department of Mechanical Engineering, G041 Lay Automotive Laboratory, University of Michigan, Ann Arbor, MI 48109 USA (corresponding author: e-mail: hpeng@umich.edu).

Norman K. Bucknor is with the General Motors R&D Center, Warren, MI 48090 USA (e-mail: Norman.k.bucknor@gm.com).

TABLE I
VEHICLE PARAMETERS OF THE PHEV-20

Vehicle	Curb weight: 1597 kg
SI Engine	2.4L, 4 Cylinder
	127kw@5300 rpm (170 hp)
	217Nm@4500 rpm (160 lb-ft)
Transmission	Automated Manual Transmission 4 speed, Gear Ratio: 2.95/1.62/1/0.68
AC Motor	Rated power: 40 kW
	Max Torque: 300 Nm
NiMH Battery	Capacity: 7.75 kw-hr
	Max Power: 40 kW
	# of Modules: 100
	Nominal Voltage: 7.5 volts/module

used, and parameters of the vehicle are summarized in Table I.

B. PHEV Model

The authors previously developed a simplified three-state HEV model to efficiently evaluate fuel economy and tail-pipe emissions for supervisory control purposes [4]. This model focuses on the effect of various engine operations on the energy flow and the catalytic converter thermal dynamics while fast dynamics (e.g. intake manifold filling and motor dynamics) are neglected. Also, low-level controls such as Air/Fuel ratio and spark timing are assumed pre-designed for optimal cold-start performance. In the state space representation, the PHEV model is described as follows.

$$\dot{x} = f(x,u) \tag{1}$$

where x is the state vector [vehicle speed, state-of-charge (SOC), and catalytic converter temperature], and u is the control input vector [engine torque, engine on/off, motor torque, gear selection, and friction brake]. Due to limited space, readers are referred to [4]-[7] for more details.

III. OPTIMAL SUPERVISORY CONTROL VIA DP

Both instantaneous and horizon optimization methods are used to solve the HEV optimal control problem for fuel economy [7]-[10]. However, optimality of the instantaneous optimization method no longer holds for PHEV optimization especially when emissions are considered. Two reasons for this are i) tailpipe emissions heavily depend on the warm-up of the catalyst temperature and ii) PHEVs are designed to significantly reduce fuel consumption by frequent and extended engine shut-downs, which may lead to catalytic converter cool-down below the light-off temperature. Therefore, a horizon-based approach must be used to solve the combined fuel and emissions optimization of the PHEV, and a DP problem is formulated and solved in the following section.

A. DP Problem Formulation

The DP problem of the PHEV is different from that of the HEV because PHEVs are designed to deplete the battery energy whereas HEVs must sustain SOC. Table II summarizes variables and their grids of the PHEV DP problem, which consists of two control inputs and two dynamic states, whereas vehicle velocity (V) and power demand (P_{dem}) are specified by the driving cycle.

TABLE II
VARIABLES AND GRID OF THE PHEV DP PROBLEM FOR FUEL AND EMISSION REDUCTION

	Variable	Grid
Stage (k)	Time	[0:1:N (final time)]
Control (u)	Engine Torque (T_{eng})	[-1, 0:5:210] Nm
	Gear (Gr)	[1 2 3 4]
State (x)	SOC	[0.2:0.01:0.9]
	Catalyst Temperature (T_{cat})	[300:40:700, 900] K

The LA-92 cycle, a high-power cycle, is selected to ensure that the engine turns on even for trips shorter than the AER, otherwise the optimal control solution is trivial (i.e. only use the battery). For extended travel distances, the LA-92, a 10 mile cycle, is repeated to generate 20 mile and 30 mile cycles, which significantly reduces computation time by reusing the cost tables during the backward optimization process. Note that the engine-off command is included in this DP problem by augmenting T_{eng} grid with -1. The friction brake command is set to maximize recuperation, and the M/G torque ($T_{m/g}$) control variable is eliminated by the drivability constraint.

$$T_{m/g} = T_{i,dem} - T_{eng} \tag{2}$$

where $T_{i,dem}$ is torque demand at the transmission input.

The optimal control problem is formulated as follows

$$\text{Minimize } J = \sum_{k=0}^{N-1} \begin{pmatrix} \alpha \cdot \max(SOC_{\min} - SOC_k, 0) + FC_k \\ + \beta \cdot HC_k + \gamma \cdot \Delta Gr^2 + \lambda \cdot \Delta E_{on/off}{}^2 \end{pmatrix} \tag{3}$$

$$\text{Subject to } \begin{aligned} & SOC_k \geq SOC_{\min} \\ & \omega_{e,\min} \leq \omega_{e,k} \leq \omega_{e,\max} \\ & T_{e,\min} \leq T_{e,k} \leq T_{e,\max} \\ & T_{M/G,\min} \leq T_{M/G,k} \leq T_{M/G,\max} \\ & P_{batt,\min} \leq P_{batt} \leq P_{batt,\max} \end{aligned} \tag{4}$$

The emission regulations emphasize eliminating cold-start HC for gasoline engines, thus let us focus on HC in this study. Due to numerical difficulties of implementing the minimum SOC constraint, the $\max(SOC_{min}-SOC_k,0)$ term is added in the cost function, and α must be adjusted to prevent SOC dropping below the minimum SOC while using electric energy as much as possible. It was found that α is quite insensitive to β, and no adjustment is necessary when all other coefficients vary. Penalties on engine on/off ($\Delta E_{on/off}$) and gear-shift (ΔGr) events are applied to improve drivability and to promote separation of engine on/off and gear selections for the extraction process in Section IV.

B. Results and Analysis

Fig. 2 shows a DP solution that balances fuel economy and emission performance for a 30 mile cycle. The optimal SOC trajectory depletes uniformly such that the final SOC barely touches the minimum SOC. Also, note that hydrocarbon emissions are kept low by fast catalyst warm-up and maintaining catalytic converter temperature (T_{cat}) above 600K to ensure high converter efficiency.

Fig. 3 shows two Pareto-curves that represent the trade-off between fuel consumption (FC) and HC for the 20 mile and 30 mile cycles. Note that the 20 mile cycle has a higher FC/HC

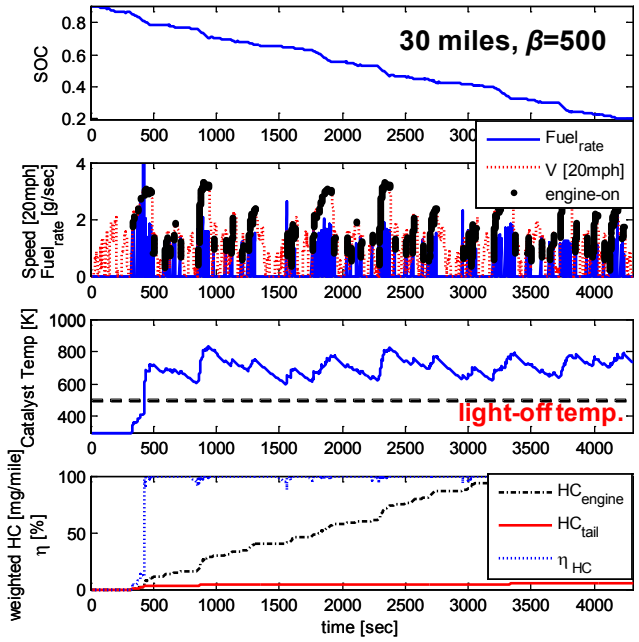

Fig. 2. DP simulation results for the 30-mile LA-92 cycle at β = 500. (α=4e3, γ=0.02, λ=0.05)

sensitivity than the 30 mile cycle and sacrifice more fuel to reduce HC. The main reason is that there is sufficient electric energy for the 20 mile cycle, and the increased engine-load and engine-on time for higher T_{cat} and conversion efficiency leads to increase in FC that was originally unnecessary when emissions were not considered. The SULEV emission standard (FTP-75 cycle) is shown as a reference.

An important trend was observed from the optimal SOC trajectories. Figure 4 shows the optimal SOC trajectory of the 30 mile cycle with respect to distance. It can be seen that SOC depletes at a constant rate when plotted on a Distance vs. SOC plane, and this holds for all SOC and distance conditions. This is an important finding because if all optimal solutions behave in this manner this slope can be used to inform the controller how much electric energy is available and how fast the battery should be depleted for optimal performance. This is the key

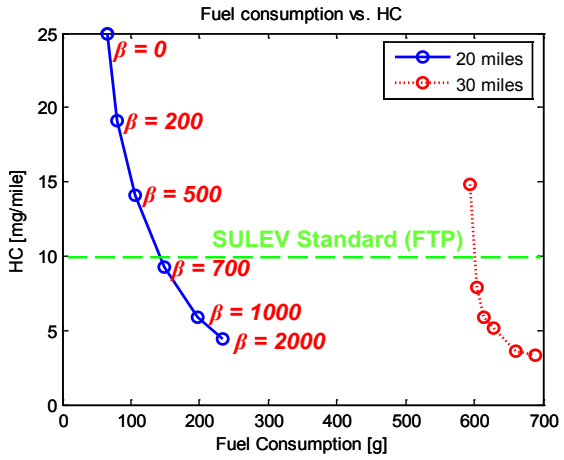

Fig. 3. Trade-off between fuel consumption and HC for 20 mile and 30 mile cycles.

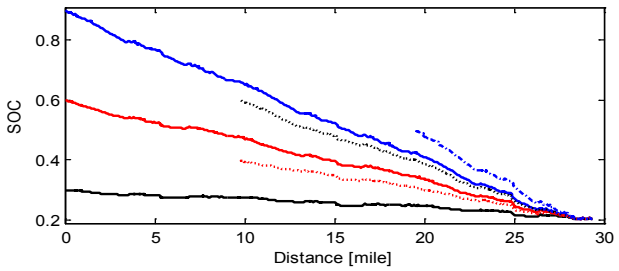

Fig. 4. Optimal SOC trajectories on a Distance vs. SOC plane.

idea of the adaptive SPC illustrated in the following sections.

IV. Comprehensive Extraction of DP Solution

A. Introduction of Energy-to-Distance Ratio (EDR)

From the previous section, we observed that the SOC vs. distance slope of the optimal solutions remain near-constant throughout the cycle. Let us quantify this slope as

$$\theta = \tan^{-1}\left(\frac{SOC - SOC_{\min}}{d_{rem}}\right) \approx \frac{SOC - SOC_{\min}}{d_{rem}} \quad (5)$$

where $\tan^{-1}$ can be removed under the small angle assumption, when the unit of distance is in miles, and SOC ranges from 0 to 1. Note that

$$\theta \le \theta_{\max} \quad (6)$$

where $\theta_{\max} = \tan^{-1}\left(\frac{0.9-0.2}{20}\right) = 0.035$ (AER=20 for PHEV20).

Thus, we can normalize θ such that

$$\bar{\theta} \equiv \frac{\theta}{\theta_{\max}} \le 1 \quad (7)$$

Note that AER and θ_{max} may change with driving style or driving cycle. Fig. 5 illustrates the Energy-to-Distance Ratio (EDR), θ, on the SOC vs. distance plane and optimal SOC trajectories for a few sample $\bar{\theta}$ values. $\bar{\theta} = 1$ indicates sufficient electric energy available (or EV mode), and $\bar{\theta} = 0$ indicates a depleted battery (or charge-sustaining mode).

B. Comprehensive Extraction Method

In an earlier study [4], a comprehensive extraction method that utilizes all of the optimal control information found from DP is proposed to learn and design the optimal cold-start strategy of HEVs. For PHEV control, this extraction method

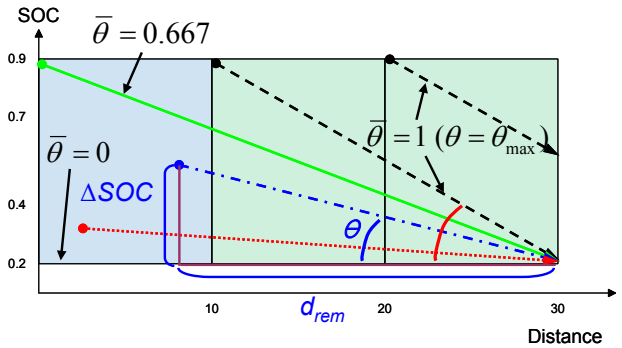

Fig. 5. Geometrical definition of EDR (θ) on the Distance vs. SOC plane.

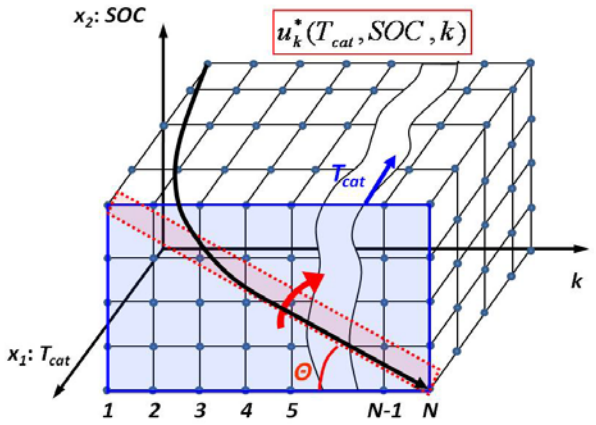

Fig. 6. State space of the optimal control policy (u_k^*) showing the two-dimensional comprehensive extraction algorithm with θ and T_{cat} sweeps.

is expanded to a two-dimensional space (EDR and T_{cat}) because the control strategy of PHEVs must be properly adjusted depending on the EDR as well as the catalyst temperature. For example, the optimal cold-start control strategy for a high EDR condition (e.g. EV mode) should be different from that for a low EDR condition (e.g. charge sustaining strategy).

Suppose that DP stores the optimal control policy in the form of $u_k^*(T_{cat}, SOC)$, where values of u_k^* are stored for all state grid points at each time step k. Then, all u_k^* elements can be grouped together by $\bar{\theta}$ and T_{cat} as shown in Fig. 6. The rectangular box represents the optimal control policy u_k^* in a state and time space, where x_1 is T_{cat} and x_2 is SOC, and k indicates the time step. Each node in the box contains the optimal control information for the given state (x_1,x_2) and time step k. The following algorithm converts u_k^* into three decoupled optimal control strategies, engine on/off ($u_{on/off}^*$), gear-shift (u_{Gear}^*), and Power Split Ratio (PSR) (u_{PSR}^*), where PSR is defined as

$$PSR \equiv \frac{P_{eng}}{P_{dem}} \tag{8}$$

Prior to the extraction algorithm, a designer must choose β that balances fuel economy and HC emissions and obtain u_k^* for the chosen β. In this study, $\beta = 500$ of the 30 mile cycle is selected for a distinct cold-start strategy. The two-dimensional extraction algorithm is described as follows:

a) Choose $T_{cat} = 300K$.
b) Let time step $k = 1$ and obtain optimal control policy u_k^*.
c) Obtain driving cycle information (P_{dem}, T_{wheel}, V, d_{rem}) at $k = 1$, where d_{rem} is the remaining distance.
d) If $T_{wheel} < 0$, store engine-off and EV gear information into $u_{on/off}^*(V, T_{wheel}, \bar{\theta}, T_{cat})$, $u_{on/off}^*(N_i, T_{dem}, \bar{\theta}, T_{cat})$, and $u_{EVGear}^*(V, P_{dem}, \bar{\theta}, T_{cat})$ matrices, and skip e) through g). Otherwise, continue to e).
e) For all SOC grid points at the chosen T_{cat}, compute $\bar{\theta}$ and convert u_k^* into two separate optimal control signals, gear selection (u_{gear}^*) and engine torque (T_{eng}^*). $u_{on/off}^*$ can be simply obtained by checking whether $T_{eng}^* = -1$ or not.
f) Find the optimal T_{dem}^* and N_i^* using u_{gear}^*, and compute $u_{PSR}^* = \frac{T_{eng}^*}{T_{dem}^*}$
g) Store all $u_{on/off}^*$, u_{PSR}^*, and u_{Gear}^* values into matrices to obtain $u_{on/off}^*(V, T_{wheel}, \bar{\theta}, T_{cat})$, $u_{on/off}^*(N_i, T_{dem}, \bar{\theta}, T_{cat})$, $u_{Gear}^*(V, P_{dem}, \bar{\theta}, T_{cat})$, and $u_{PSR}^*(N_i, T_{dem}, \bar{\theta}, T_{cat})$.
h) Repeat b) through g) for all time steps k.
i) Repeat a) through h) for all other T_{cat}.

C. Extracted Results

1) Hot DP results ($T_{cat} > 700K$): Although two sets of optimal control strategies (hot and cold) are extracted, only cold strategy is presented in this paper due to limited space. Readers are referred to the previous paper for hot strategy [3].

2) Cold DP results ($T_{cat} < 700K$): Four sets of the optimal control strategies under $\bar{\theta} = [0.02 \quad 0.35 \quad 0.6 \quad 0.97]$ at T_{cat} = 420K are selected and plotted in Figs. 7-9. In general, the cold-start strategy of the PHEV is found to be similar to that of the conventional HEV [4]. In fact, low-EDR results are almost identical to those of conventional HEVs because low-EDR solution is an optimal charge sustaining strategy, but the transition of hot-to-cold strategy takes place gradually and starts at a higher temperature than the catalyst light-off temperature. With increasing $\bar{\theta}$, more interesting results are observed as follows.

Figure 7 shows that the engine on/off should be triggered by both the transmission input speed and driver power demand when the catalyst cools down. While the transmission input speed threshold stays constant throughout the range of $\bar{\theta}$, the power threshold increases with increasing $\bar{\theta}$. Figure 8 indicates that late-shift strategy is desired for higher exhaust gas temperature and fast catalyst warm-up during cold-starts. Readers are referred to the previous paper by the authors for engine maps [4]. Again, the low $\bar{\theta}$ results are identical to those of conventional HEVs, and this late-shift strategy does not significantly change with increasing $\bar{\theta}$ except for the increased engine on/off threshold. For the cold-start power-split strategy, Fig. 9 shows that another PSR line should be used to reproduce optimal power-split strategy during cold-starts for higher exhaust gas temperature, which promotes faster catalyst warm-up.

V. Optimal Supervisory Control via DP

Assuming that the remaining distance information is available, the design and evaluation of the cold-start SPC for the PHEV are carried out as follows. Two cold SPCs (Map-based and DP-based) are developed for catalyst temperature management. These cold SPCs are compared with DP results under various EDR conditions.

A. Hot SPC Algorithm: Adaptive DP-based SPC

Based on the extracted hot results, the logic of the adaptive

Hot SPC algorithm is proposed as follows.

If $P_{dem}<P_{on/off}(\bar{\theta})$,

Turn off the engine and select the gear using the Electric Vehicle (EV) shift-map.

$P_{m/g} = P_{dem}$

If V<60mph, then disengage the clutch for engine disconnect

Else, engage the clutch.

Else,

Turn on the engine

Select the gear using the engine-on mode shift-map and find T_{dem} *and* N_i

Find PSR using T_{dem} *and* N_i *and compute* $P_{eng} = PSR \cdot P_{dem}$

Compute M/G power: $P_{m/g} = P_{dem} - P_{eng}$

End

The flow chart of the above DP-based SPC algorithm is illustrated in Fig. 10 to help visualize the logic. Note that $P_{on/off}$ threshold and shift-map are functions of $\bar{\theta}$, and they can be found from the previous paper [3]. Other non-adaptive design parameters, *PSR* map and EV shift-map, are also used. In this algorithm, the engine on/off power, gear shifting map, and *PSR* commands are sequentially determined because the *PSR* decision requires T_{dem} and N_i, which can only be determined after gear selection is made, and the shift-map selection depends on the engine on/off decision. Embedding DP information in this rule-based control structure provides decoupled control logics of three sub-control modules: engine on/off, shift, and *PSR*, and is expected to perform near optimally.

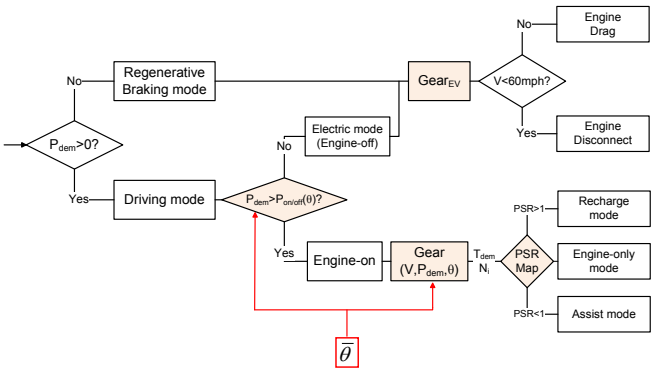

Fig. 10. Flowchart of the adaptive DP-based SPC.

B. *Cold SPC Algorithm*

1) Map-based Cold SPC: The Map-based Cold SPC is an instantaneous optimization method, previously developed by the authors for the fast catalyst warm-up of conventional HEVs [4]. Since tail-pipe emissions are primarily determined by the catalyst light-off, the idea of the Map-based Cold SPC is to find the optimal throttle and shift strategy that minimizes engine-out HC but maximizes the exhaust gas temperature for fast catalyst warm-up using transient (corrected) engine maps. Again, due to limited space readers are referred to the

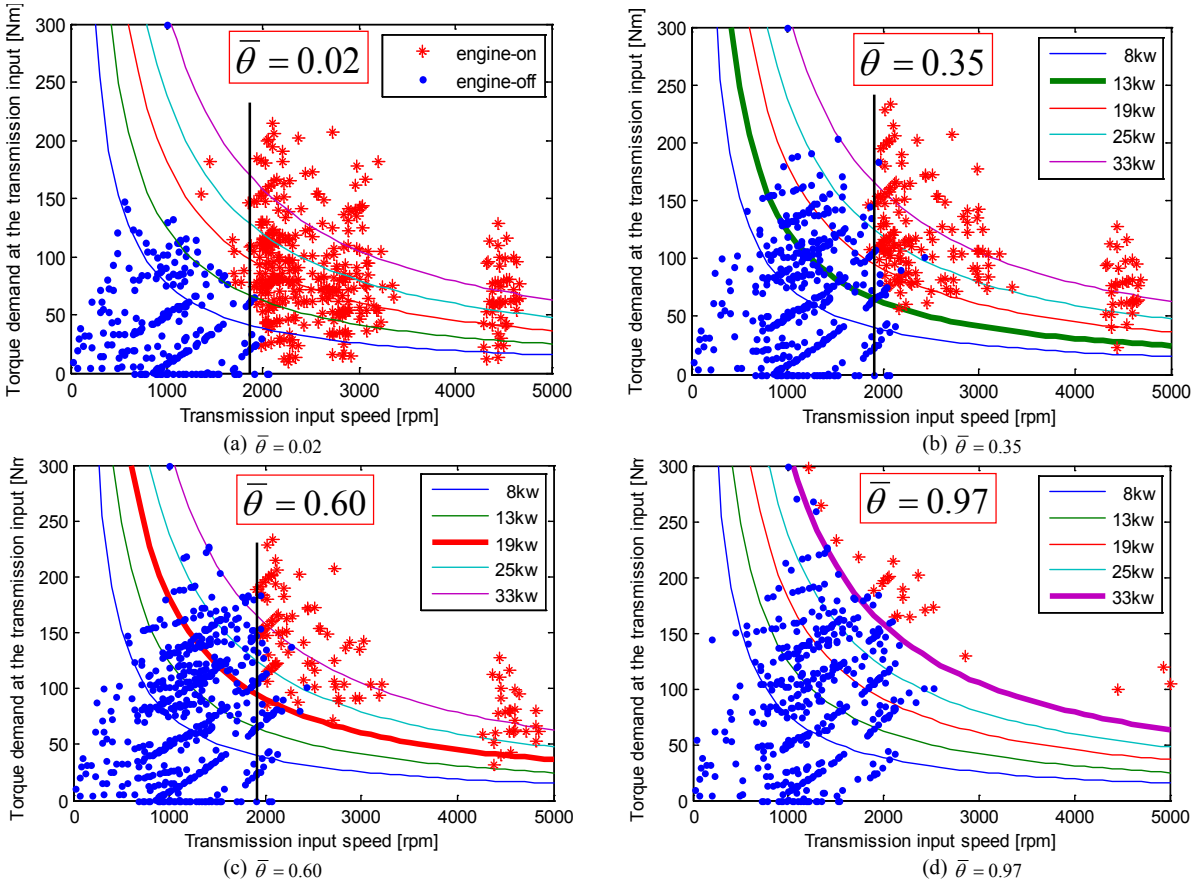

Fig. 7. Extracted cold-catalyst engine on/off strategies at four sample $\bar{\theta}$ values.

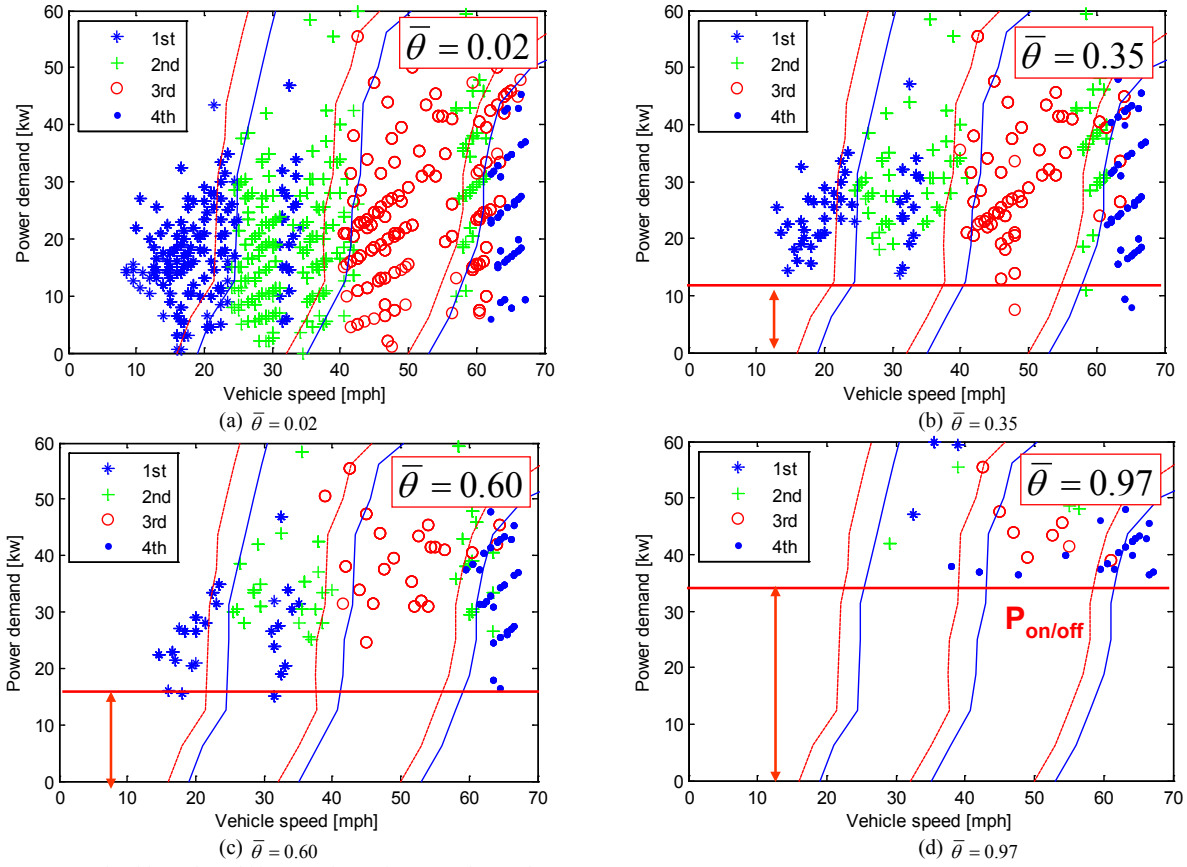

(a) $\bar{\theta} = 0.02$ (b) $\bar{\theta} = 0.35$ (c) $\bar{\theta} = 0.60$ (d) $\bar{\theta} = 0.97$

Fig. 8. Extracted cold-catalyst shift strategies at four sample $\bar{\theta}$ values.

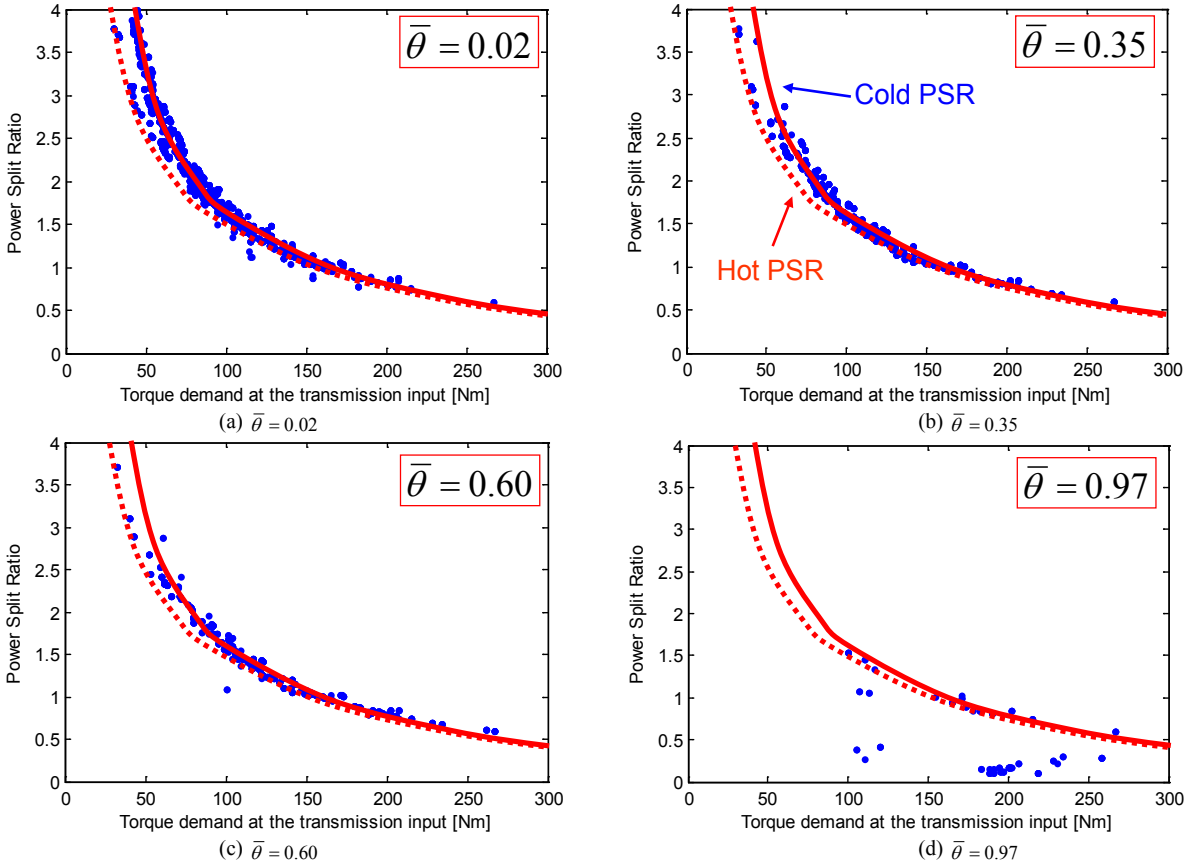

(a) $\bar{\theta} = 0.02$ (b) $\bar{\theta} = 0.35$ (c) $\bar{\theta} = 0.60$ (d) $\bar{\theta} = 0.97$

Fig. 9. Extracted cold-catalyst power-split strategies at four sample $\bar{\theta}$ values.

cold-start HEV study for the optimization algorithm [4].

2) DP-based Cold SPC: The DP-based Cold SPC is simply using a set of cold maps in the proposed DP-based Hot SPC algorithm (Fig. 10) except for the engine on/off algorithm. The engine on/off logic of the Cold SPC is triggered by both the transmission input speed (N_i) and power demand (P_{dem}), where the power threshold is adjusted based on $\bar{\theta}$.

C. *Results and Discussion* (*Cold SPC algorithms*)

For a fair comparison of the DP-based vs. Map-based Cold SPC, both controllers share the adaptive DP-based Hot SPC so that the control strategy is different only during the cold transient. Also, the cost function of the DP problem is used to evaluate combined fuel economy and emissions performance.

First, the DP-based Cold SPC is implemented, and its simulation responses are compared with DP solution. Figure 11 indicates that cold DP results are successfully extracted and the control signals and vehicle states of the DP-based SPC are very similar to those of DP. For cold-start performance evaluation, Fig. 12 shows that the DP-based SPC outperforms the Map-based SPC under various $\bar{\theta}$ conditions. The main reason for the inferior performance of the Map-based SPC is its engine on/off strategy because the Map-based optimization method is unable to determine when the engine should be turned on/off during a cold-start, and thus the engine on/off algorithm of the DP-based Hot SPC is used for the Map-based Cold SPC.

VI. Conclusion

This paper studies the simultaneous optimization of fuel economy and emissions for Plug-in HEVs under various travel distance and SOC conditions. In order to quantify the level of SOC with respect to the remaining distance, the variable

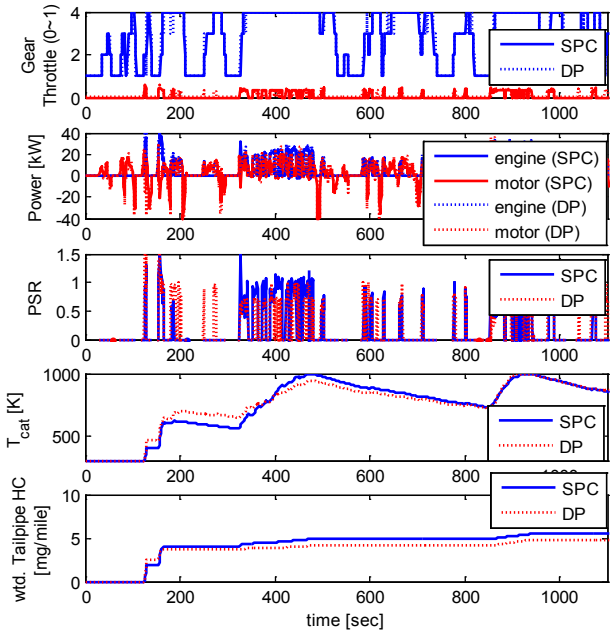

Fig. 11. Simulation response comparison of DP vs. DP-based SPC for $\bar{\theta}=0.381$ on the cold-start LA92 cycle.

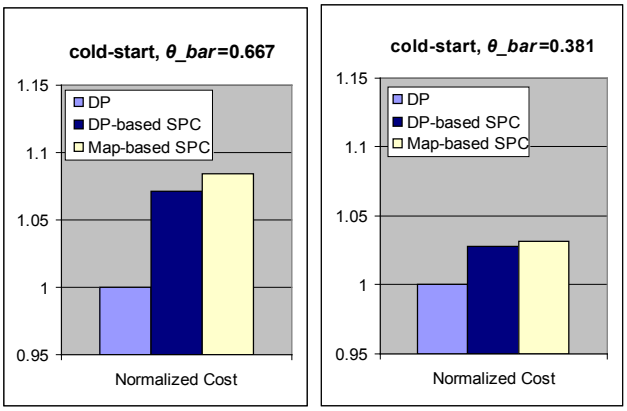

Fig. 12. FC and HC combined performance comparison of DP, Map-based SPC, and DP-based SPC for various $\bar{\theta}$ on the cold-start LA92 cycle.
*Cost function: $J = FC(g) + 500 \cdot HC(g)$

Energy to Distance Ratio (EDR), θ, is introduced and used to extract key control strategies from the DP solutions. The extracted results indicate that the supervisory controller must be properly adjusted depending on EDR and the catalyst temperature. In particular, for the pre-transmission parallel configuration, engine on/off and gear-shift strategies play key roles in the adaptive optimal charge management by controlling the engine speed and consequently the electric energy flow, while the power-split strategy mainly focuses on optimizing the engine efficiency for the given engine speed.

Acknowledgment

The authors would like to thank General Motors R&D's Propulsion Systems Research Lab for supporting this project.

References

[1] J. Gonder, and T. Markel, "Energy management strategies for plug-in hybrid electric vehicles," *SAE*, paper 2007-01-0290, 2007.

[2] P. Sharer, A. Rousseau, D. Karbowski, and S. Pagerit, "Plug-in hybrid electric vehicle control strategy: comparison between EV and charge-depleting options," *SAE*, paper 2008-01-0460, 2008.

[3] D. Kum, H. Peng, and N. Bucknor, "Optimal control of plug-in HEVs for fuel economy under various travel distances," *IFAC Advances in Automotive Control Conference*, Munich, Germany, 2010.

[4] D. Kum, H. Peng, and N. Bucknor, "Supervisory control of parallel hybrid electric vehicles for fuel economy and emissions," *ASME Trans. on Dynamic Systems, Measurement, and Control*, in press.

[5] G. Rizzoni, Y. Guezennec, A. Brahma, X. Wei, and T. Miller, "VP-SIM: A unified approach to energy and power flow modeling simulation and analysis of hybrid vehicles," *SAE*, paper 2000-01-1565, 2000.

[6] A. Rousseau, S. Pagerit, G. Monnet, and A. Feng, "The new PNGV System Analysis Toolkit PSAT V4.1 – evolution and improvement," *SAE*, paper 2001-01-2536, 2001.

[7] C.-C. Lin and H. Peng, "Power management strategy for a parallel hybrid electric truck," *IEEE Trans. on Control Systems Technology*, vol. 11, no. 6, pp. 839-849, 2003.

[8] J. Liu and H. Peng, "Modeling and control of a power-split hybrid vehicle," *IEEE Trans. on Control Systems Technology*, vol. 16, no. 6, pp. 1242-1251, 2008.

[9] P. Pisu and G. Rizzoni, "Comparative study of supervisory control strategies for hybrid electric vehicles," *IEEE Trans. on Control Systems Technology*, vol. 15, no. 3, pp. 506-518, 2007.

[10] A. Sciarretta and L. Guzzella, "Control of hybrid electric vehicles: optimal energy-management strategies," *IEEE Control Systems Magazine*, vol. 27, no. 2, pp. 60-70, 2007.